

Continuous-wave laser operation of Tm and Ho co-doped NaY(WO₄)₂ and NaLu(WO₄)₂ crystals

X. Han,¹ F. Fusari,² M. D. Serrano,¹ A. A. Lagatsky,^{2,3} J. M. Cano-Torres,¹
C. T. A. Brown,² C. Zaldo^{1,*} and W. Sibbett²

¹ Instituto de Ciencia de Materiales de Madrid. Consejo Superior de Investigaciones Científicas.
c/ Sor Juana Inés de la Cruz 3. 28049 Madrid, Spain

² School of Physics and Astronomy, University of St. Andrews, St. Andrews, KY16 9SS, UK

³aal2@st-andrews.ac.uk

*cezaldo@icmm.csic.es

Abstract: Tetragonal single crystals of NaT(WO₄)₂ (T = Y or Lu) co-doped with Tm³⁺ and Ho³⁺ ions have been employed for broadly tunable and efficient room-temperature laser operation at around 2 μm. With Ti:sapphire laser pumping at 795 nm, a slope efficiency and a maximum output power as high as 48% and 265 mW, respectively, have been achieved at 2050 nm from a Tm,Ho:NaY(WO₄)₂ crystal. Tuning from 1830 nm to 2080 nm has also been obtained using an intracavity Lyot filter.

©2010 Optical Society of America

OCIS codes: (140.5680) Rare earth and transition metal solid-state lasers; (160.5690) Rare-earth-doped materials; (140.3600) Lasers, tunable.

References and links

1. C. Cascales, M. D. Serrano, F. Esteban-Betegón, C. Zaldo, R. Peters, K. Petermann, G. Huber, L. Ackermann, D. Rytz, C. Dupre, M. Rico, J. Liu, U. Griebner, and V. Petrov, "Structural, spectroscopic, and tunable laser properties of Yb³⁺-doped NaGd(WO₄)₂," *Phys. Rev. B* **74**(17), 174114 (2006).
2. A. García-Cortés, J. M. Cano-Torres, X. Han, C. Cascales, C. Zaldo, X. Mateos, S. Rivier, U. Griebner, V. Petrov, and F. J. Valle, "Tunable continuous wave and femtosecond mode-locked Yb³⁺ laser operation in NaLu(WO₄)₂," *J. Appl. Phys.* **101**(6), 063110 (2007).
3. A. García-Cortés, J. M. Cano-Torres, M. D. Serrano, C. Cascales, C. Zaldo, S. Rivier, X. Mateos, U. Griebner, and V. Petrov, "Spectroscopy and lasing of Yb-doped NaY(WO₄)₂: Tunable and femtosecond mode-locked laser operation," *IEEE J. Quantum Electron.* **43**(9), 758–764 (2007).
4. J. M. Cano-Torres, M. D. Serrano, C. Zaldo, M. Rico, X. Mateos, J. Liu, U. Griebner, V. Petrov, F. J. Valle, M. Galán, and G. Viera, "Broadly tunable laser operation near 2 μm in a locally disordered crystal of Tm³⁺-doped NaGd(WO₄)₂," *J. Opt. Soc. Am. B* **23**(12), 2494–2502 (2006).
5. X. Han, J. M. Cano-Torres, M. Rico, C. Cascales, C. Zaldo, X. Mateos, S. Rivier, U. Griebner, and V. Petrov, "Spectroscopy and efficient laser operation near 1.95 μm of Tm³⁺ in disordered NaLu(WO₄)₂," *J. Appl. Phys.* **103**(8), 083110 (2008).
6. M. Rico, J. M. Cano-Torres, M. D. Serrano, C. Cascales, C. Zaldo, U. Griebner, and V. Petrov, "Tunable, continuous-wave near 2-μm laser operation of Tm³⁺ in NaY(WO₄)₂ single crystal," in *Advanced Solid-State Photonics* (Optical Society of America, Washington, DC, 2009), WB27.
7. W. B. Cho, A. Schmidt, J. H. Yim, S. Y. Choi, S. Lee, F. Rotermund, U. Griebner, G. Steinmeyer, V. Petrov, X. Mateos, M. C. Pujol, J. J. Carvajal, M. Aguiló, and F. Díaz, "Passive mode-locking of a Tm-doped bulk laser near 2 microm using a carbon nanotube saturable absorber," *Opt. Express* **17**(13), 11007–11012 (2009).
8. A. A. Lagatsky, F. Fusari, S. Calvez, J. A. Gupta, V. E. Kisel, N. V. Kuleshov, C. T. A. Brown, M. D. Dawson, and W. Sibbett, "Passive mode locking of a Tm,Ho:KY(WO₄)₂ laser around 2 microm," *Opt. Lett.* **34**(17), 2587–2589 (2009).
9. H. Wang, J. Li, G. Jia, Z. You, F. Yang, Y. Wei, Y. Wang, Z. Zhu, X. Lu, and C. Tu, "Optical properties of Ho³⁺-doped NaGd(WO₄)₂ crystal for laser materials," *J. Alloy. Comp.* **431**(1–2), 277–281 (2007).
10. A. Méndez-Blas, M. Rico, V. Volkov, C. Zaldo, and C. Cascales, "Crystal field analysis and emission cross sections of Ho³⁺ in the locally disordered single-crystal laser hosts M⁺Bi(XO₄)₂ (M⁺=Li, Na; X=W, Mo)," *Phys. Rev. B* **75**(17), 174208 (2007).
11. B. M. Walsh, "Review of Tm and Ho materials; spectroscopy and lasers," *Laser Phys.* **19**(4), 855–866 (2009).
12. A. A. Lagatsky, F. Fusari, S. V. Kurilchik, V. E. Kisel, A. S. Yasukevich, N. V. Kuleshov, A. A. Pavlyuk, C. T. A. Brown, and W. Sibbett, "Optical spectroscopy and efficient continuous-wave operation near 2 μm for a Tm,Ho:KYW laser crystal," *Appl. Phys. B* **97**(2), 321–326 (2009).

1. Introduction

Inhomogeneously broadened single crystals doped with rare-earth ions have received significant attention as promising gain media for construction of compact, efficient and broadly tunable solid-state lasers operating in near-infrared region. The tetragonal ($I\bar{4}$ space group) double tungstates with nominal formula $\text{NaT}(\text{WO}_4)_2$ (NaTW), where Na and T = Y, La-Lu are monovalent and trivalent cations, respectively, are a class of disordered crystals where the inhomogeneous properties arise from the quasi-random occupancy of two nonequivalent lattice sites ($2b$ and $2d$) by Na and T cations [1]. These crystals, when doped with Yb^{3+} ions, have been studied comprehensively in recent past years and this has led to the demonstration of a range of sub-100 fs modelocked lasers operating in the 1- μm spectral region [2,3].

More recently, these studies have been extended to Tm^{3+} -doped NaTW (T = Gd, La, Lu, and Y) crystals with the aim of developing efficient and broadly tunable lasers that operate around 2 μm [4–6]. Indeed, for the $\text{Tm}:\text{NaYW}$ crystal the tunability range extended from 1850 nm to 2030 nm with spectral widths at half maximum (FWHM) of 110 nm and 142 nm for π - and σ -polarizations, respectively [6]. It follows that such gain media can also be employed for ultrashort-pulse generation using appropriate modelocking techniques [7,8]. Ultrafast laser sources around 2 μm are of particular interest for applications in time-resolved spectroscopy, nonlinear frequency up-conversion to the mid/far-infrared spectral regions, mid-IR supercontinuum generation, optical communications and photomedicine. With Ho^{3+} as a co-doping active ion, tunable laser operation in a somewhat longer wavelength range extending to ~ 2.1 μm ($^5\text{I}_7 \rightarrow ^5\text{I}_8$) can be obtained and this is preferred in remote sensing because of lower atmospheric absorption. Also, Ho^{3+} ions are generally characterised by higher emission cross-sections and longer upper laser level lifetimes compared to their Tm^{3+} counterparts and these features are especially desirable for low-threshold and efficient laser operation.

Here we report on crystal growth, spectroscopy and room-temperature continuous-wave laser operation for Tm^{3+} and Ho^{3+} co-doped NaYW and NaLuW crystals in the 2 μm spectral region. Evidence of an enhancement of the tuning range in Tm,Ho co-doped NaTW crystals as compared to their singly-doped Tm^{3+} counterparts has been demonstrated.

2. Crystal growth

NaYW single crystals were grown in air by the Czochralski method using platinum (Pt) crucibles. Details of the growth procedures can be found in previously reported work [3]. Two different sets of Tm,Ho co-doped crystals were grown with 5 at% Tm^{3+} concentration in the melt and with two Ho^{3+} concentrations of 0.25 at% and 0.5 at%. Oriented (001) seeds of $\text{NaY}(\text{WO}_4)_2$ were used in both cases.

A $\text{Tm}(5\text{at\%}),\text{Ho}(0.5\text{at\%}):\text{NaLuW}$ crystal was grown by the top seeded solution growth (TSSG) method using a Pt crucible. A $\text{Na}_2\text{WO}_4\text{-Na}_2\text{W}_2\text{O}_7$ mixture in molar ratio 1:1 was used as flux, and the solute-to-flux molar ratio was 1:9. The seed was a (001)-oriented $\text{Tm}(5\text{at\%}):\text{NaLuW}$ crystal. The growth started by melting and homogenization at 910 $^\circ\text{C}$ over a period of one day. The saturation temperature was found to be 880 $^\circ\text{C}$. The crystal growth proceeded at this temperature for one week and afterwards the melt was cooled down to 842 $^\circ\text{C}$ at a 0.05 $^\circ\text{C}/\text{h}$ cooling rate. The crystal was extracted from the melt and cooled to 745 $^\circ\text{C}$ at 4 $^\circ\text{C}/\text{h}$ and later to room temperature (RT) at a rate of 15 $^\circ\text{C}/\text{h}$.

For both growth methods, the $\text{Tm},\text{Ho}:\text{NaY}(\text{Lu})\text{W}$ compounds and flux were synthesized using precursors of 99.5% Na_2CO_3 , 99.8% WO_3 , 99.99% Y_2O_3 (Alfa Aesar), 99.99% Lu_2O_3 , 99.99% Tm_2O_3 and 99.99% Ho_2O_3 (WuXi YiFeng Rare Earth Co LTD). The crystalline samples were oriented by the Laue X-ray method, then cut as (100) oriented plates and polished to optical quality.

3. Optical spectroscopy

The optical absorption spectra of the investigated crystals in the visible and near-infrared spectral regions for σ (E \perp c,B \parallel c) and π (E \parallel c,B \perp c) polarisations were recorded using a Varian

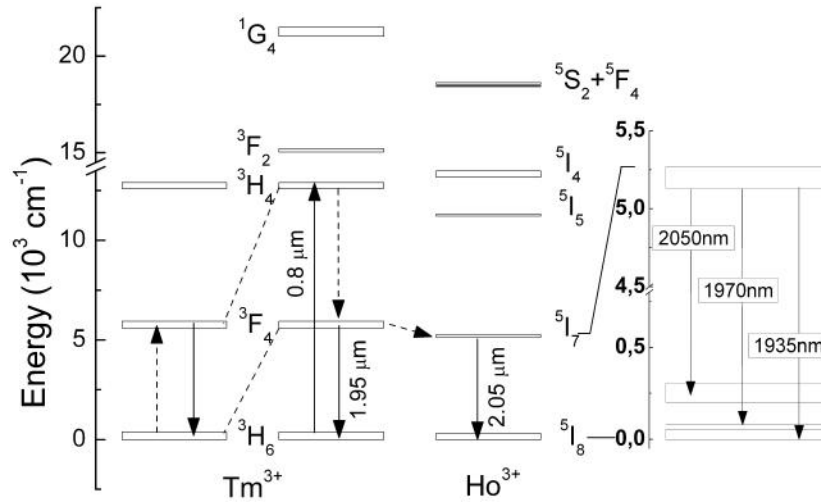


Fig. 1. Simplified energy level diagrams for Tm^{3+} and Ho^{3+} lanthanides. The continuous arrows show absorption and emission transitions, while dashed arrows show non-radiative transitions and energy transfer processes.

(Cary 5E) spectrophotometer. Figure 1 shows a diagram of the Ho^{3+} and Tm^{3+} energy levels relevant to the subsequent discussion of the results. For most of the spectral ranges, the Ho^{3+} and Tm^{3+} RT optical absorption bands overlap, but at around 540 nm the Ho^{3+} ($5\text{I}_8 \rightarrow 5\text{S}_2 + 5\text{F}_4$) absorption is free of Tm^{3+} lines (Fig. 2). Advantage was taken of this fact to evaluate the Ho^{3+} concentration in the crystals considering the integrated absorbance of Ho^{3+} in the isostructural NaGdW [9] crystal as a reference. By contrast, the Ho^{3+} absorption in the spectral region from 840 nm to 760 nm is negligible [10] and the corresponding Tm^{3+} ($3\text{H}_6 \rightarrow 3\text{H}_4$) optical absorption band can be used for the evaluation of the Tm^{3+} concentration in the grown crystals using a previously investigated $\text{Tm}(5\text{at}\%):\text{NaYW}$ crystal for the reference data [6]. In Table 1 the calculated Tm^{3+} and Ho^{3+} concentrations are summarized for the crystalline samples used.

Table 1. Tm^{3+} and Ho^{3+} concentrations in the melt and in the crystal.

Crystal	Growth method	$[\text{Tm}^{3+}]_{\text{melt}}$ (at%)	$[\text{Ho}^{3+}]_{\text{melt}}$ (at%)	$[\text{Tm}^{3+}]_{\text{crystal}}$ (10^{20}cm^{-3} – at%)	$[\text{Ho}^{3+}]_{\text{crystal}}$ (10^{20}cm^{-3} – at%)
NaY(WO ₄) ₂	CZ	5	0.25	3.07 – 4.68	0.19 – 0.29
		5	0.5	3.07 – 4.68	0.31 – 0.47
NaLu(WO ₄) ₂	TSSG	5	0.5	3.92 – 5.86	0.86 – 1.28

The Tm^{3+} optical absorption in both crystals at around 800 nm ($3\text{H}_6 \rightarrow 3\text{H}_4$) was characterized by a strong anisotropy, with the strongest absorption band observed for σ -polarisation centered at 795.5 nm (Fig. 2). The optical absorption for π -polarisation was less than a half that of the σ -value at around 795 nm with the existence of a secondary maximum at 781 nm.

Figure 3 shows the RT emission of Tm and Ho co-doped NaYW and NaLuW crystals when excited at 795.5 nm using a Ti:sapphire laser. It can be seen that the Tm emission covers efficiently the 1600–2000 nm region ($3\text{F}_4 \rightarrow 3\text{H}_6$ transition; see for comparison the emission spectra of $\text{Tm}:\text{NaYW}$ Fig. 3(b)). Additionally, two well resolved bands peaking at 1944 nm and 2049 nm were observed in all of the studied samples. These bands could be attributed to

the $^5I_7 \rightarrow ^5I_8$ Ho^{3+} transition (the emission of Ho^{3+} in isostructural $\text{NaBi}(\text{WO}_4)_2$ is included in Fig. 3(a) for comparison) and these were found to be less sensitive to the polarization configurations of the samples. These transitions are excited by Tm-Ho energy transfer [11] which is favored by the large cut-off phonon energy of these double tungstates hosts,

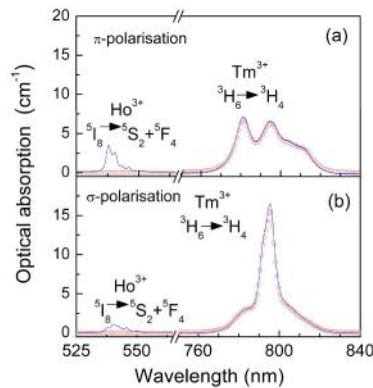


Fig. 2. RT optical absorption of Tm(5at%), Ho(0.5at%):NaLuW (blue continuous line) and absorption of Tm(5at%):NaLuW (red pointed line is given for comparison) for (a) π - and (b) σ -polarizations.

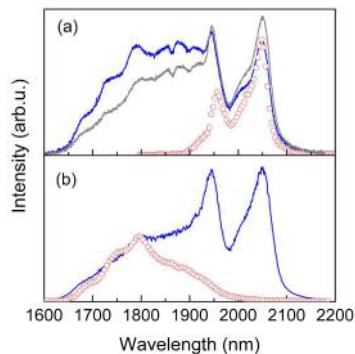


Fig. 3. (a) RT unpolarized emission of Tm(5at%), Ho(0.25at%):NaYW (blue line) and Tm(5at%), Ho(0.5 at%):NaYW (grey line); (b) Tm(5at%), Ho(0.5at%): NaLu(WO₄)₂ (blue line). The $(2\sigma + \pi)/3$ averaged emission cross sections of Ho:NaBiW and Tm:NaYW are included as red circles in (a) and (b), respectively.

typically $\hbar\omega = 900\text{-}1000 \text{ cm}^{-1}$. It can be seen that the relative intensity of the Ho^{3+} emission increases as the Ho/Tm concentration ratio increases (see Fig. 3).

4. Laser results

Assessment of the lasing performance of the Tm,Ho co-doped NaYW and NaLuW crystals was undertaken with the V-type astigmatically-compensated resonator shown in Fig. 4. This set up comprised two curved mirrors (radii of curvature of -75 mm and -100 mm) designed for high transmission at the pump wavelength ($T > 98\%$) and high reflectivity in the 1800-2100 nm range together with an output coupler OC with either 1% or 2% transmission at around 2000 nm. The cavity was configured to provide a mode radius of $25 \mu\text{m}$ inside the gain crystal. A Ti:sapphire laser providing 1.15 W of power at 794.5 nm was used as a pump source and its beam was focused into the gain medium by a 50 mm focal length lens to a spot radius of $23.5 \mu\text{m}$ ($1/e^2$ intensity) measured in the air at the location of the gain crystal. All of the samples were (100)-cut uncoated Brewster-angled plates maintained at $20 \text{ }^\circ\text{C}$ by using a Peltier-cooled Cu sample holder to which samples were glued with a silver paste. The

absorption of the sample was also measured in situ (during lasing) by detecting transmitted pump power. To maintain a similar absorption for the σ and π laser assessments, the sample thickness in the latter case (π) was approximately twice that of the former (σ).

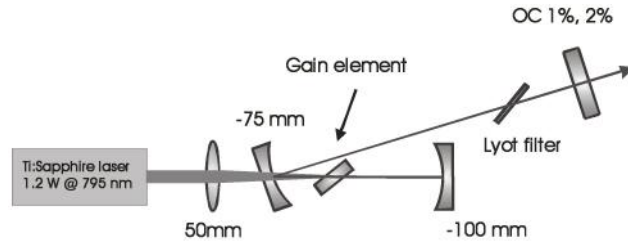


Fig. 4. Experimental laser set-up.

4.1 *Tm,Ho:NaY(WO₄)₂ crystals*

The NaYW crystals co-doped with 5 at% Tm and 0.25 at% or 0.5 at% Ho and oriented in the cavity for pumping/lasing in σ - or π -polarizations were used during continuous-wave (cw) laser experiments. Figure 5 depicts the summary of the laser results obtained with the Tm(5at%),Ho(0.25at%):NaYW crystals. The maximum slope efficiency $\eta = 48\%$ was obtained in a 1.55-mm-long crystal (σ -polarisation) with a 2% output coupling (Fig. 5(a)). The corresponding maximum average output power was 240 mW and the laser threshold was reached at 55 mW of absorbed pump power. Slightly lower efficiencies were recorded when a 3.36-mm-long crystal was used in a π -configuration, namely, $\eta = 43\%$ and $\eta = 39\%$ for 2% and 1% OCs, respectively. Interestingly, the maximum output power reached 265 mW due to a higher level of absorbed pump power at π -polarisation (1.55-mm-long and 3.36-mm-long crystals absorbed in ranges of 80-70% and 85-77% of pump radiation for σ - and π -polarizations, respectively, depends on pump power level).

It should be noted that dual wavelength operation was observed in the case of the 1.55-mm-long Tm,Ho:NaYW crystal (σ -polarization). Additional to the output at 2050 nm, laser emissions at 1935 nm or 1970 nm were observed when the pump power reached a sufficiently high level (300 mW for 1% OC). This can be explained by the quasi-three-level nature of the $\text{Ho}^{3+} {}^5\text{I}_7 \rightarrow {}^5\text{I}_8$ transition - see Fig. 1. The ${}^5\text{I}_8$ Ho ground multiplet has a first set of Stark levels at 0-50 cm^{-1} , an isolated level at 79 cm^{-1} , followed by an energy gap of $\approx 120 \text{ cm}^{-1}$ [10]. At low pump powers the laser transition favors the high-energy Stark levels of the ${}^5\text{I}_8$ manifold (low reabsorption losses), but at increased pump power the lower Stark levels become saturated thereby permitting lasing in these channels. This explains why an additional lasing band did not arise around 1935 nm or 1970 nm in the case of 3.36-mm-thick samples were reabsorption losses are larger such that higher pump power levels would be required to reach transparency.

A similar laser performance was observed for the Tm(5at%),Ho(0.5at%):NaYW crystal as compared to the 0.25 at% Ho-doped counterpart. Notably, slope efficiencies as high as 37% were achieved with corresponding maximum output powers of up to 230 mW at 2058 nm (Fig. 6). A more pronounced roll-over of input-output characteristics can be observed with the 0.5at% Ho-doped samples compared to the lower-doped counterparts. This fact can be explained by the presence of up-conversion losses in the Tm-Ho system [12]. Indeed, during quasi-cw operation (10% duty cycle) involving the Tm(5at%),Ho(0.5at%):NaYW crystal a slope efficiency as high as 43% was measured for the π -polarization and this is comparable to the values obtained for lower Ho-doped samples during cw operation.

Tunable operation of the Tm,Ho:NaYW lasers was obtained by inserting a 2-mm thick Lyot filter into the long cavity arm and the results obtained with the Tm(5at%),Ho(0.25at%):NaYW crystal are as summarized in Fig. 7. Tuning to $\sim 2080 \text{ nm}$ was observed whereas a high energy stop-band varied from 1825 nm for 1.55-mm-long crystal to 1880 nm for 3.5-mm-long. All crystals with higher Ho^{3+} -doping and 3.4-mm-long 0.25 at% Ho-doped

element produced maximum output powers at around 2050 nm whereas the σ -polarized 0.25 at% Ho-doped crystal was characterized by a flatter tuning profile in the 1950-2050 nm range and this could be advantageous for ultrashort pulse generation.

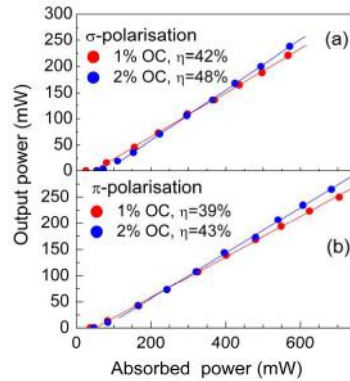


Fig. 5. Cw laser performance of Tm(5at%), Ho(0.25at%):NaYW crystal. (a) σ -pol. (1.55-mm-long crystal). (b) π -pol. (3.4-mm-long crystal).

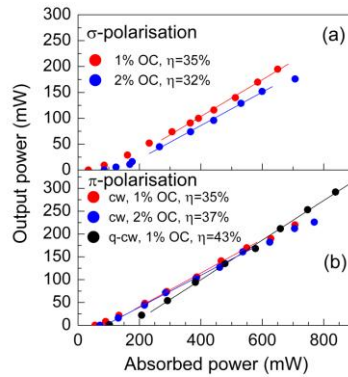


Fig. 6. Cw and quasi cw laser performance of the Tm (5at%),Ho(0.5at%):NaYW crystals. (a) σ -pol. (1.75-mm-long crystal). (b) π -pol. (3.5-mm-long crystal).

4.2 Tm,Ho:NaLu(WO₄)₂ crystals

All Tm(5at%),Ho(0.5at%):NaLuW crystal samples (1.46-mm and 2.7-mm long for σ and π , respectively) investigated produced laser emission only around 2060 nm in the absence of any tuning element in the cavity. The performance was characterized by quite pronounced thermal effects, more evident as the absorbed pump power increased. As a representative example, Fig. 8(a) depicts an output power vs pump characteristic for a cw and a quasi-cw operation (10% duty cycle) for σ -polarization. Only 50 mW of average power was achieved during cw operation, whereas a slope efficiency up to 47% was reached with a chopped pump.

A similar tuning range of 2020-2070 nm was demonstrated for all Tm,Ho:NaLuW samples. This is much narrower than the tuning ranges observed for Tm,Ho:NaYW crystals (see Figs. 7 and 8(b)). The difference between both cases is due first to a more efficient Tm-Ho energy transfer associated to the higher Tm and Ho concentrations in NaLuW, which prevents optical gain at Tm³⁺ (1850-2020 nm lasing range). Secondly, pronounced thermal roll-over in input-output characteristics of Tm,Ho:NaLuW indicates about higher heat load in this laser crystal, likely due to enhanced probability of up-conversion in the Tm-Ho system, the nature of which should be further investigated. On this reason the tunability range is

limited to ~2020-2070 nm since the lower Ho^{3+} levels at $\sim 0\text{-}50\text{ cm}^{-1}$ and $\sim 80\text{ cm}^{-1}$ become thermally populated making the Ho laser transitions in $\sim 1900\text{-}2000\text{ nm}$ range too lossy.

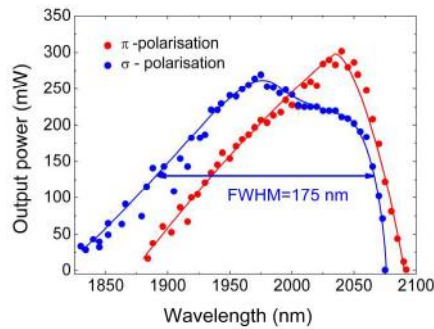


Fig. 7. Tunability of the Tm(5at%),Ho(0.25at%):NaYW crystal for σ - and π -polarizations. The sample thickness for σ and π were 1.55 mm and 3.4 mm, respectively.

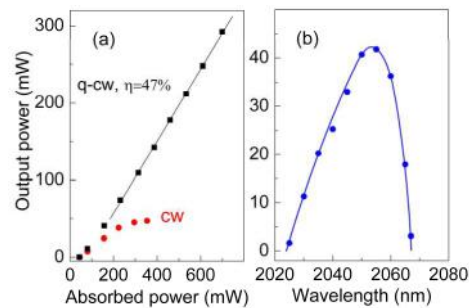


Fig. 8. Laser performance of the Tm(5at%), Ho(0.5at%):NaLuW crystal. (a) Input-output characteristics during cw (red points) and quasi-cw operation (black squares). (b) Cw tunability for the σ -polarization (1.46-mm-long crystal).

5. Conclusions

Continuous-wave and broadly tunable laser operation of the Tm,Ho co-doped $\text{NaY}(\text{WO}_4)_2$ crystals around $2\ \mu\text{m}$ has been demonstrated with Ti:sapphire laser pumping at 795 nm. Maximum slope efficiencies of 48% and 43% with corresponding output powers of 240 mW and 265 mW were realized around 2050 nm using a Tm(5at%),Ho(0.25at%) co-doped crystal in σ - and π -configurations, respectively. It has also been deduced that the specific distribution of the $^5\text{I}_8\text{ Ho}^{3+}$ Stark energy levels in Tm,Ho:NaYW crystals leads to competition between several $^5\text{I}_7 \rightarrow ^5\text{I}_8(n)$ laser channels. While emission at 2050 nm is always observed, a second laser band (either at 1970 nm or 1935 nm) can be obtained simultaneously when the lowest levels becomes partially depopulated at high pump levels, thereby producing a dual-wavelength operation. When an intracavity Lyot filter was used for tuning experiments an output from 1830 nm to 2075 nm with a FWHM of 175 nm and a top-hat profile was observed that favors femtosecond pulse generation when a laser of this type is modelocked.

Acknowledgments

Work supported by projects (Spain) MAT2008-06729-C02-01 and (UK) EP/D04622X/1.